All-Optical Measurement of High-Harmonic Amplitudes and Phases in Aligned Molecules

A. Rupenyan,[1] J. B. Bertrand,[2] D. M. Villeneuve,[2] and H. J. Wörner[1,*]

[1]*Laboratorium für Physikalische Chemie, ETH Zürich, Wolfgang-Pauli-Strasse 10, 8093 Zürich, Switzerland*

[2]*Joint Laboratory for Attosecond Science, National Research Council of Canada and University of Ottawa, 100 Sussex Drive, Ottawa, Canada, K1A0R6*

(Received 4 October 2011; published 20 January 2012)

We report a new all-optical approach to measuring the phase and amplitude of high-harmonic emission from aligned molecules. We combine the transient grating technique with a continuous rotation of the molecular alignment axis and develop an analytical model that enables the simultaneous determination of phases and amplitudes. Measurements in N_2 molecules are shown to be in qualitative agreement with the results of *ab initio* quantum scattering calculations.

DOI: 10.1103/PhysRevLett.108.033903 PACS numbers: 42.65.Ky, 33.20.Xx, 33.80.Wz, 42.50.Hz

High-harmonic generation (HHG) spectroscopy is sensitive to molecular structure and dynamics, encoded in the amplitudes and phases of the emitted radiation. It constitutes a new method to access ultrafast nuclear and electronic motion triggered by strong-field ionization [1,2] and ultrafast molecular dynamics occurring in photochemical reactions [3–5]. In a typical HHG experiment, an electron is tunnel ionized from the target molecule by a strong laser field, driven away from it, and finally recombines with it. The energy gained during the acceleration of the electron is emitted upon recombination in the form of high harmonics in the extreme ultraviolet (XUV) spectral range [6]. This emission, from a gas phase sample of aligned molecules, contains information about the electronic structure of the molecule through the amplitudes and phases of the photorecombination matrix elements [7,8]. Achieving a detailed characterization of the electronic structure and dynamics through HHG requires a complete measurement of amplitudes and phases in the molecular frame. Although spectral amplitudes in molecular HHG have been studied in great detail, the determination of the phase of the emitted harmonics still remains a challenge.

Previous measurements of high-harmonic phases in aligned molecules have used gas mixtures [9–11], two-source interference [12], the reconstruction of attosecond beating by interference of two-photon transitions (RABBITT) [13,14] or simply the temporal variation of the observed amplitudes [15]. The measurements with gas mixtures, as well as pure amplitude measurements are unavoidably affected by the assumed shape of the molecular axis distribution to obtain both phase and amplitude. The measurements using the RABBITT technique provide phase and amplitude as a function of the photon energy but cannot relate phases for different molecular alignment angles.

In this Letter we demonstrate a new all-optical approach to measuring simultaneously and self-consistently the amplitude and phase of high-harmonic emission from aligned molecules by combining the transient grating technique [16] with a continuous rotation of the polarization of the two grating beams. We use the randomly aligned sample as a local oscillator against which we coherently detect the emission from the aligned molecules. We develop a fully analytical formalism to separate the contributions from amplitudes and phases and determine them directly. Our technique relies on a simple purely optical experimental setup. It provides the phase as a function of alignment angle for each harmonic order and is thus complementary to the RABBITT technique. The combination of our technique with either RABBITT or mixed gas experiments would provide the high-harmonic phase as a function of photon energy *and* alignment angle [17]. We apply the method to aligned N_2 molecules and compare them with accurate quantum scattering calculations. High-harmonic generation gives access to the phase of photorecombination matrix elements, which is hard to measure otherwise. Our results enable the first comparison between high-harmonic phase as a function of angle and quantitative scattering calculations [8].

The experiment uses a chirped-pulse amplified titanium-sapphire femtosecond laser, a high-harmonic source chamber equipped with a pulsed valve and an XUV spectrometer. The laser beam, comprising 8-mJ pulses of 32-fs duration (full-width at half-maximum, FWHM) centered at 800 nm, is split into two parts of variable intensities using a half-wave plate and a polarizer. The major part (probe) is sent through a computer-controlled delay stage towards the high-harmonic chamber, while the minor part (pump) is temporally stretched by means of SF6 glass and sent through a 50:50 beam splitter to generate two equally intense 800-nm pulses. The two pump beams are aligned parallel to the probe beam with a vertical offset of ± 1.5 cm, and the three beams are focused into the high-harmonic chamber using an $f = 50$ cm spherical mirror. The pump pulses set up a transient grating of alignment in the vertical direction (x) and the probe pulse generates high-order harmonics that are spectrally dispersed in the horizontal plane (zy) by a concave grating whereas the

beam freely diverges in the vertical direction [Fig. 1(a)]. The periodic structure of the medium results in partial diffraction of the high harmonics. The spectrally resolved far-field harmonic profiles are detected with a microchannel plate detector backed with a phosphor screen and recorded with a charge-coupled device camera. For the measurements as a function of the alignment angle, the polarization of the two pump beams is rotated by means of a zero-order $\lambda/2$ wave plate [Fig. 1(b)]. The typical pulse energies amount to 1 mJ (probe beam) and 330 μJ (pump beams), resulting in respective intensities of 2×10^{14} W/cm^2 and 0.66×10^{14} W/cm^2 in the bright zones of the grating. Neat N_2 is introduced into the high-harmonic source chamber by means of a pulsed nozzle with a 100 μm diameter and a backing pressure of 3–4 bars.

In the transient grating geometry, the intensity of the alignment field is periodically modulated across the sample in the transverse (x) direction. In our experiments, the pump intensity and degree of axis alignment ($\langle\cos^2\theta\rangle$) are linearly related [18], resulting in a sinusoidal alignment grating [Fig. 1(b)]. Consequently, we parametrize the high-harmonic emission from the transient grating at photon energy Ω in terms of a combined amplitude and phase grating modulating between $d_\Omega^{\mathrm{iso}} \exp(i\phi_\Omega^{\mathrm{iso}})$, for randomly distributed molecules, and $d_\Omega^{\theta} \exp(i\phi_\Omega^{\theta})$, for the ensemble of molecules aligned by a laser pulse of polarization forming an angle θ with respect to the laser field generating the high harmonics [19]. The electric field of high-harmonic emission across the grating is thus given by

$$E(\Omega, x) = [d_\Omega^{\mathrm{iso}} + (d_\Omega^{\theta} - d_\Omega^{\mathrm{iso}}) f(x)] \times \exp[i\{\phi_\Omega^{\mathrm{iso}} + (\phi_\Omega^{\theta} - \phi_\Omega^{\mathrm{iso}}) f(x)\}] \quad (1)$$

where $f(x) = (\sin(kx) + 1)/2$ and $k = 2\pi/\Lambda$ with $\Lambda = 13.3$ μm is the period of the grating. At each photon energy Ω, the observed signal is normalized to the emission from the randomly-aligned sample, $F(\Omega, x) = E(\Omega, x)/(d_\Omega^{\mathrm{iso}} e^{i\phi_\Omega^{\mathrm{iso}}})$, which serves as a reference for the definition of the relative phases ($\phi_\Omega = \phi_\Omega^{\theta} - \phi_\Omega^{\mathrm{iso}}$) and amplitudes ($d_\Omega = d_\Omega^{\theta}/d_\Omega^{\mathrm{iso}}$). In the far field, where the high harmonics are detected, the observed signal corresponds to the (squared modulus of the) Fourier transform of $F(\Omega, x)$ which is [20]

$$FT_{x\to\xi}\{F(\Omega, x)\} = e^{i\phi_\Omega/2} \sum_{m=-\infty}^{\infty} \{(1 + (d_\Omega - 1)/2) J_m(\phi_\Omega/2) + i(d_\Omega - 1)/4[J_{m+1}(\phi_\Omega/2) - J_{m-1}(\phi_\Omega/2)]\} \delta\left(\xi - m\frac{k}{2\pi}\right), \quad (2)$$

where ξ is the transverse (x-direction) spatial frequency and k has been defined above. The far-field signal thus consists of nondiffracted ($m = 0$) and diffracted ($m \neq 0$) parts for each harmonic photon energy Ω, with amplitudes determined by linear combinations of Bessel functions J_m with arguments given by half the phase-modulation depth. Measuring the intensity in the $m = 0$ and $m = \pm 1$ orders thus fully determines the amplitude modulation and the absolute value of the phase-modulation depth for each harmonic order which can thus be determined directly from the experiment. In the present analysis, we focus on the component of HHG emission parallel to the driving field. The perpendicular component adds a weak orthogonal contribution to the detected intensities, which could be separated in future experiments using an XUV polarizer. In the present experiments, we have not observed higher-order diffraction ($|m| > 1$) because the alignment intensity was kept low.

Figure 2(a) shows the yield of harmonic 19 in both the zero-order and the first-order diffraction. This

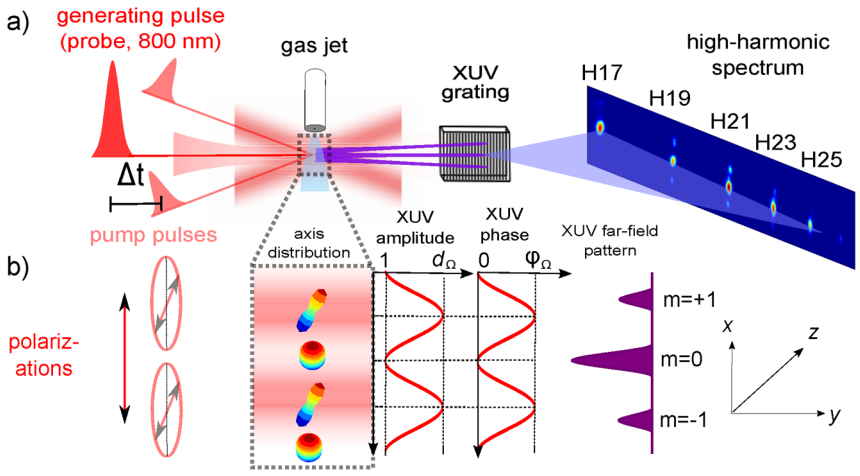

FIG. 1 (color online). (a) Experimental setup for high-harmonic transient grating spectroscopy with aligned molecules. (b) Distribution of the combined intensity of the pump pulses in the transient grating and near-field modulation of the amplitudes and phases of high-harmonic emission leading to diffraction in the far field.

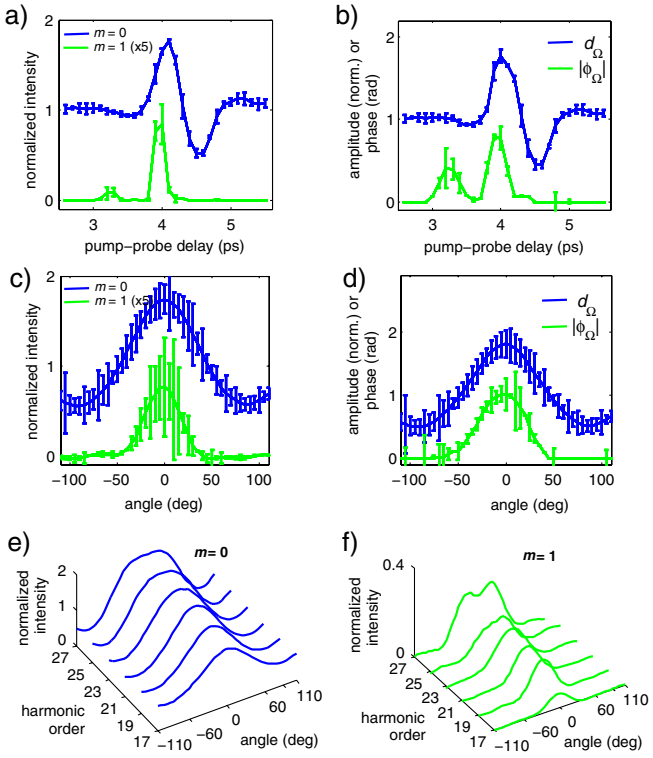

FIG. 2 (color online). (a) Evolution of the normalized intensities of H19 in the zero-order and the first-order diffraction side band with pump-probe delay, measured in N_2. (b) Reconstructed relative amplitude and phase of H19, referenced to an isotropically aligned sample. (c) Undiffracted ($m = 0$) and diffracted ($m = 1$) intensities of the high-harmonic emission as a function of the alignment angle measured at a pump-probe delay of 4.1 ps. (d) Reconstructed relative high-harmonic amplitudes and phases as a function of the alignment angle. (e),(f) Evolution of the normalized intensities of harmonics 17 to 27 in the zero order (e) and the first-order (f) diffraction side band with alignment angle, measured at $\Delta t = 4.1$ ps.

measurement has been performed with an alignment angle $\theta = 0°$ (i.e., the polarizations of the pump and probe pulses are parallel), around the first rotational half revival, centered at 4.1 ps. The error bars represent the 95% confidence intervals of the measured intensities. The intensity of the zeroth order follows the well-known pattern of a maximum of emission when molecules are parallel to the generating laser polarization, followed by a minimum corresponding to antialigned molecules, and return to isotropic distribution [21,22]. The $m = 1$ harmonic yield has a global maximum at the time of maximal alignment, and a weak local maximum preceding it. Both the $m = 0$ and the $m = 1$ yields have been divided by the $m = 0$ signal at negative delays, corresponding to an isotropic distribution of the N_2 molecules.

Figure 2(b) shows the high-harmonic phase and amplitude of H19, relative to a sample of randomly aligned molecules, extracted from the data in Fig. 2(a) using Eq. (2). The amplitude essentially follows the evolution of the $m = 0$ intensity. In contrast, the phase modulates more sharply and shows a larger peak preceding the main revival, compared to the one observed in $m = 1$. The error bars on the amplitude and phase are obtained by error propagation.

We now turn to measurements as a function of angle, fixing the pump-probe delay to 4.1 ps and rotating the polarization of both alignment beams. Figure 2(c) shows the yields of harmonic 19 in $m = 0$ and $m = 1$. Here, we have normalized the data (both $m = 0$ and $m = 1$) measured at an alignment angle of 0° to the $m = 0$ data point corresponding to maximal alignment in the pump-probe delay measurement shown in Fig. 2(a). The intensity of the $m = 0$ component is maximal when the alignment axis is parallel to the polarization of the generating pulse (0°) and minimal when it is perpendicular (90°). The diffracted $m = 1$ component follows the same trend but modulates much more sharply with a vanishing intensity for alignment angles in the range of 50–90°. The error bars are 95% confidence intervals. The extracted amplitude and phase as a function of alignment angle is shown in Fig. 2(d). The amplitude again essentially follows the modulation of the $m = 0$ component whereas the phase has a narrower angular dependence. The error bars on the amplitude and phase are obtained by error propagation.

Figures 2(e) and 2(f) show the yields of the harmonic orders 17–27 as a function of the alignment angle in $m = 0$ (e) and $m = 1$ (f). The angular variation of the intensities is found to broaden with increasing harmonic order. The angular variation of the $m = 1$ signal is narrower than that of the corresponding $m = 0$ signal, but also broadens with increasing harmonic order. The magnitude of the intensity variations in both components decreases around 0° with increasing harmonic order, with an essentially flat top in $m = 0$ for H27 and even a local minimum in $m = 1$. As we show below, this observation can be attributed to the angular variation of the phase of the photorecombination matrix element.

We now proceed to comparing the experimentally retrieved amplitudes and phases of the high harmonics from the alignment-dependence measurements, with *ab initio* quantum scattering calculations, using ePolyScat [23,24] with orbitals from a Hartree-Fock calculation using a correlation-consistent valence-triple-zeta (cc-pVTZ) basis set. Figures 3(a) and 3(b) show the molecular-frame photorecombination amplitudes (a) and phases (b) as a function of alignment angle for harmonic orders 13–41. In this calculation only the highest-occupied molecular orbital (HOMO) has been taken into account. These calculations agree well with those reported in Ref. [8]. We have further multiplied the complex photorecombination dipoles with the square root of the ionization yield from [25] and convoluted the result with an alignment distribution corresponding to $\langle \cos^2\theta \rangle = 0.55$, taken from Ref. [26]. Finally, the result has been divided by the

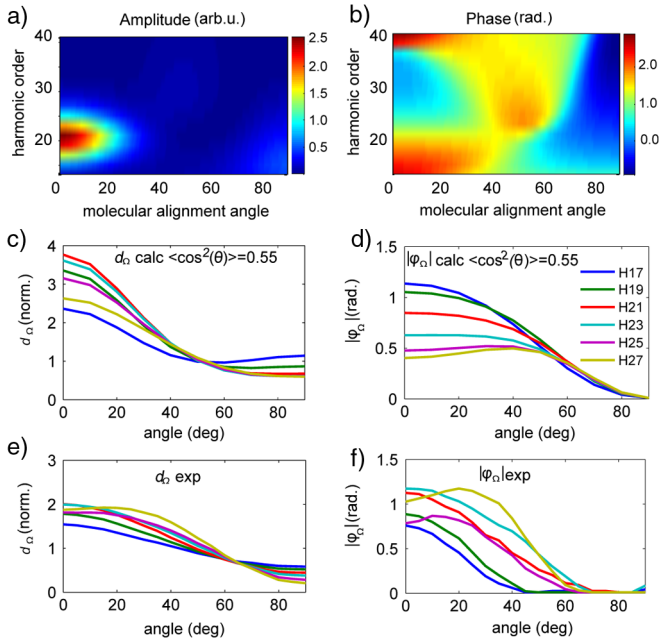

FIG. 3 (color online). (a),(b) Calculated amplitudes and phases of the molecular-frame photoionization matrix elements of N_2. (c),(d) Calculated high-harmonic amplitudes and phases using an alignment distribution characterized by $\langle\cos^2(\theta)\rangle = 0.55$. The phases have been set to zero at $\theta = 90°$. (e),(f) High-harmonic amplitudes and phases reconstructed from the experiment on N_2.

calculated complex emission dipole of a randomly aligned sample and is displayed in Figs. 3(c) and 3(d). The error in these predicted amplitudes and phases is dominated by the lack of knowledge about the axis alignment distribution, which cannot easily by measured in HHG experiments. By using alignment distribution functions in the range $\langle\cos^2\theta\rangle = 0.50$–$0.60$, we estimate the error in the calculated amplitudes and phases to amount to $\pm 20\%$ [19].

The angular variations of the amplitudes and phases of harmonics 17 to 27, extracted from the experimental data shown in Figs. 2(e) and 2(f) using Eq. (2) are shown in Figs. 3(e) and 3(f). The experimental error is on the order of 20% in the amplitudes and on the order of ± 0.15 rad in the phases, similar to what is shown in Fig. 2(d). Although the amplitude and phase modulations are slightly overestimated in the theoretical prediction, they follow in magnitude and shape the experimentally retrieved amplitude and phase modulations. The increase of the amplitude modulation vs angle with harmonic order and the intersection of the curves close to 60° is also correctly reproduced. The experimentally observed broadening of the phase variation with increasing harmonic order is reproduced in the calculated phases. The local minima at $\theta = 0°$ in the phases of H25 and H27 are also correctly predicted by the calculations, although the positions of the local maxima in these harmonic orders differ somewhat. Taking the uncertainties discussed above into account, we thus obtain a reasonable agreement between the calculated and observed variations of high-harmonic amplitudes and phases.

We now discuss the origin of the observed amplitude and phase variations by comparing them to the theoretical results. The large local maximum appearing in Fig. 3(a) around H21 for small angles is the known shape resonance occurring in the photoionization from the $3\sigma_g$ HOMO of N_2 to the σ_u photoelectron continuum [27]. This shape resonance causes the angular variation of the relative high-harmonic amplitude shown in panel c to increase from H17 to H21, an effect that is also observed in the experimental results in panel e. The shape resonance is also responsible for a rapid phase variation across its center, which is clearly visible in panel b. This effect causes the angular variation of the phase to change from a simple monotonic step function with extrema at 0° and 90° for harmonic orders 17 and 19 to nonmonotonic functions with pronounced maxima in the range of 40–60° for higher harmonic orders. In the relative high-harmonic phases shown in panel d this evolution translates into the appearance of a local minimum at 0° for H25 and H27, which agrees with the experimental observations.

Although the experimental and theoretical results agree reasonably well overall, some discrepancies remain. Most notably, the experimentally obtained phases decay to zero at smaller angles than the predicted ones and the ordering of the curves in panels (d) and (f) do not coincide. The agreement of the amplitudes is better but the experimental results are systematically smaller than the theoretical ones. Possible sources of error are the fact that we have neglected the component of high-harmonic emission perpendicular to the polarization generating pulse in the present analysis or the fact that the laser electric field is neglected in the quantum scattering calculations. Both aspects need to be improved in future studies.

The phases of the high harmonics emitted from N_2 have previously been observed with the RABBITT technique [14]. However, since the latter cannot measure phases as a function of alignment angle, the phase of harmonic 17 has been assumed to be angle independent. Both the present measurements and the calculations show that the phase modulation for all harmonics in the measured range is on average 0.5 rad or more, with a small increase from harmonic order 17 to 27. We do observe a significant phase modulation in harmonics 25 and 27, in contrast to a previous report where the diffraction of these orders was unresolved [18]. These examples show the need for accurate measurements of the high-harmonic phases as a function of angle. The good agreement between calculated and experimentally retrieved harmonic amplitudes and phases justifies the choice of considering only the HOMO in the present work. Indeed, the next lower orbital, HOMO-1, has been reported to only play a role at high intensities and in the highest harmonics [28,29]. In another multiorbital

analysis [30], a cancellation of several HHG emission channels has been predicted, which explained the fact that the observed intensities and ellipticities agree well with calculations including only the HOMO [31].

In conclusion, we have demonstrated a new all-optical method for measuring amplitudes and phases in aligned molecules simultaneously and self-consistently. The results of such a measurement can be used to perform a coherent deconvolution of the high-harmonic observables by calculating or measuring the molecular axis distribution. This approach would give access to molecular-frame amplitudes and phases that could then be compared directly with theoretical models. Our method is complementary to the RABBITT technique [13,14] by measuring phases and amplitudes as a function of alignment angle, rather than as a function of photon energy. The combination of the two techniques would provide two-dimensional amplitudes and phases in addition to data redundancy that would enable an additional verification of self-consistency. The recently developed techniques of time-resolved high-harmonic spectroscopy measure phases and amplitudes of transient species as a function of time, relative to unexcited molecules, which serve as a local oscillator [3–5]. Such measurements will ideally be extended to aligned molecular samples, in which case the phase and amplitude of the emission from unexcited aligned molecules will need to be determined. The present approach thus represents a powerful addition to such techniques and will enable molecular-frame measurements of the electronic structure of transient species.

We gratefully acknowledge funding from the Swiss National Science Foundation (PP00P2_128274), ETH Zürich (ETH-33 10-3 and Postdoctoral Fellowship Program) and the Marie Curie COFUND program.

*woerner@phys.chem.ethz.ch
www.atto.ethz.ch

[1] S. Baker, J. S. Robinson, C. A. Haworth, H. Teng, R. A. Smith, C. C. Chirila, M. Lein, J. W. G. Tisch, and J. P. Marangos, Science **312**, 424 (2006).
[2] H. Niikura, H. J. Wörner, D. M. Villeneuve, and P. B. Corkum, Phys. Rev. Lett. **107**, 093004 (2011).
[3] H. J. Wörner, J. B. Bertrand, D. V. Kartashov, P. B. Corkum, and D. M. Villeneuve, Nature (London) **466**, 604 (2010).
[4] H. J. Wörner, J. B. Bertrand, P. B. Corkum, and D. M. Villeneuve, Phys. Rev. Lett. **105**, 103002 (2010).
[5] H. J. Wörner *et al.*, Science **334**, 208 (2011).
[6] P. B. Corkum, Phys. Rev. Lett. **71**, 1994 (1993).
[7] H. J. Wörner, H. Niikura, J. B. Bertrand, P. B. Corkum, and D. M. Villeneuve, Phys. Rev. Lett. **102**, 103901 (2009).
[8] A.-T. Le, R. R. Lucchese, S. Tonzani, T. Morishita, and C. D. Lin, Phys. Rev. A **80**, 013401 (2009).
[9] N. Wagner, X. Zhou, R. Lock, W. Li, A. Wüest, M. Murnane, and H. Kapteyn, Phys. Rev. A **76**, 061403 (2007).
[10] T. Kanai, E. J. Takahashi, Y. Nabekawa, and K. Midorikawa, Phys. Rev. A **77**, 041402(R) (2008).
[11] B. K. McFarland, J. P. Farrell, P. H. Bucksbaum, and M. Gühr, Phys. Rev. A **80**, 033412 (2009).
[12] X. Zhou, R. Lock, W. Li, N. Wagner, M. M. Murnane, and H. C. Kapteyn, Phys. Rev. Lett. **100**, 073902 (2008).
[13] W. Boutu *et al.*, Nature Phys. **4**, 545 (2008).
[14] S. Haessler *et al.*, Nature Phys. **6**, 200 (2010).
[15] C. Vozzi, M. Negro, F. Calegari, G. Sansone, M. Nisoli, S. De Silvestri, and S. Stagira, Nature Phys., **7**, 822 (2011)
[16] Y. Mairesse, D. Zeidler, N. Dudovich, M. Spanner, J. Levesque, D. M. Villeneuve, and P. B. Corkum, Phys. Rev. Lett. **100**, 143903 (2008).
[17] J. B. Bertrand, H. J. Wörner, P. Salières, P. B. Corkum, and D. M. Villeneuve (to be published).
[18] Y. Mairesse, N. Dudovich, D. Zeidler, M. Spanner, D. M. Villeneuve, and P. B. Corkum, J. Phys. B **43**, 065401 (2010).
[19] See Supplemental Material at http://link.aps.org/supplemental/10.1103/PhysRevLett.108.033903, where we have checked that amplitudes and phases vary linearly with $\langle \cos^2\theta \rangle$ in the range of 0.33-0.55.
[20] The derivation is given in the Supplemental Material in [19].
[21] T. Kanai, S. Minemoto, and H. Sakai, Nature (London) **435**, 470 (2005).
[22] J. Itatani, D. Zeidler, J. Levesque, M. Spanner, D. M. Villeneuve, and P. B. Corkum, Phys. Rev. Lett. **94**, 123902 (2005).
[23] F. A. Gianturco, R. R. Lucchese, and N. Sanna, J. Chem. Phys. **100**, 6464 (1994).
[24] A. P. P. Natalense and R. R. Lucchese, J. Chem. Phys. **111**, 5344 (1999).
[25] D. Pavičić, K. F. Lee, D. M. Rayner, P. B. Corkum, and D. M. Villeneuve, Phys. Rev. Lett. **98**, 243001 (2007).
[26] C. Jin, A.-T. Le, and C. D. Lin, Phys. Rev. A **83**, 053409 (2011).
[27] J. L. Dehmer, D. Dill, and S. Wallace, Phys. Rev. Lett. **43**, 1005 (1979).
[28] B. K. McFarland, J. P. Farrell, P. H. Bucksbaum, and M. Gühr, Science **322**, 1232 (2008).
[29] G. H. Lee, I. J. Kim, S. B. Park, T. K. Kim, Y. S. Lee, and C. H. Nam, J. Phys. B **43**, 205602 (2010).
[30] Y. Mairesse *et al.*, Phys. Rev. Lett. **104**, 213601 (2010).
[31] A.-T. Le, R. R. Lucchese, and C. D. Lin, Phys. Rev. A **82**, 023814 (2010).

Supplementary Material for
All-optical measurement of high-harmonic amplitudes and phases in aligned molecules

A. Rupenyan, J. B. Bertrand, D. M. Villeneuve, and H. J. Wörner, *

1. MODELING AND ANALYSIS OF HIGH-HARMONIC EMISSION FROM TRANSIENT GRATINGS OF ALIGNED MOLECULES

As described in the Letter, the electric field of high-harmonic emission across the transient grating, normalized to the emission of isotropically aligned molecules, is given by

$$\begin{aligned} F(\Omega,x) &= \left[1+\frac{d_\Omega-1}{2}(\sin(kx)+1)\right]\exp\left[i\frac{\phi_\Omega}{2}\{\sin(kx)+1\}\right] \\ &= \left[1+\frac{d_\Omega-1}{2}\sin(kx)+\frac{d_\Omega-1}{2}\right]\exp\left(i\frac{\phi_\Omega}{2}\right)\exp\left[i\frac{\phi_\Omega}{2}\sin(kx)\right] \\ &= \exp\left(i\frac{\phi_\Omega}{2}\right)\left[(1+\frac{d_\Omega-1}{2})\exp\left(i\frac{\phi_\Omega}{2}\sin(kx)\right)+\frac{d_\Omega-1}{2}\sin(kx)\exp\left(i\frac{\phi_\Omega}{2}\sin(kx)\right)\right]. \end{aligned} \tag{1}$$

In the far field, the signal corresponds to the squared modulus of the Fourier transform of $F(\Omega,x)$ with the spatial frequency ξ

$$\mathcal{F}_{x\to\xi}\{F(\Omega,x)\}=\exp\left(i\frac{\phi_\Omega}{2}\right)\sum_{m=-\infty}^{\infty}\left[(1+\frac{d_\Omega-1}{2})J_m(\frac{\phi_\Omega}{2})+i\frac{d_\Omega-1}{4}\{J_{m+1}(\frac{\phi_\Omega}{2})-J_{m-1}(\frac{\phi_\Omega}{2})\}\right]\delta(\xi-m\frac{k}{2\pi}). \tag{2}$$

Here, J_m stands for the m-th order Bessel functions. The analytical form of the Fourier transform has been derived using the following relations,

$$\mathcal{F}\{\sin(kx)\} = \frac{i}{2}\{\delta(\xi+\frac{k}{2\pi})-\delta(\xi-\frac{k}{2\pi})\} \tag{3}$$

$$\mathcal{F}\{\exp(i\frac{\phi_\Omega}{2}\sin(kx))\} = \sum_{m=\infty}^{-\infty}J_m(\frac{\phi_\Omega}{2})\delta(\xi-m\frac{k}{2\pi}) \tag{4}$$

and applying the convolution theorem $\mathcal{F}(A.B)=\mathcal{F}(A)^*\mathcal{F}(B)$:

$$\begin{aligned} \mathcal{F}\{\sin(kx)\exp(i\frac{\phi_\Omega}{2}\sin(kx))\} &= \mathcal{F}\{\sin(kx)\}*\mathcal{F}\left[\exp\{i\frac{\phi_\Omega}{2}\sin(kx)\}\right] \\ &= \frac{i}{2}\{\delta(\xi+\frac{k}{2\pi})-\delta(\xi-\frac{k}{2\pi})\}*\sum_{m=-\infty}^{\infty}J_m(\frac{\phi_\Omega}{2})\delta(\xi-m\frac{k}{2\pi}) \\ &= \frac{i}{2}\sum_{m=-\infty}^{\infty}\left[J_{m+1}(\frac{\phi_\Omega}{2})-J_{m-1}(\frac{\phi_\Omega}{2})\right]\delta(\xi-m\frac{k}{2\pi}). \end{aligned} \tag{5}$$

The periodic modulation of the high-harmonic amplitude and phase in the near field results in several diffraction orders in the far field. The observed intensity distribution in the far field is the power spectrum of Eq. (2) which means that the zeroth order (or non-diffracted) high-harmonic signal has the intensity at the detector

$$I_{m=0}=\left|(1+\frac{d_\Omega-1}{2})J_0(\frac{\phi_\Omega}{2})+i\frac{d_\Omega-1}{4}\{J_1(\frac{\phi_\Omega}{2})-J_{-1}(\frac{\phi_\Omega}{2})\}\right|^2. \tag{6}$$

The first order signal has the intensity

$$I_{m=1}=\left|(1+\frac{d_\Omega-1}{2})J_1(\frac{\phi_\Omega}{2})+i\frac{d_\Omega-1}{4}\{J_2(\frac{\phi_\Omega}{2})-J_0(\frac{\phi_\Omega}{2})\}\right|^2. \tag{7}$$

Supplementary Material for
All-optical measurement of high-harmonic amplitudes and phases in aligned molecules

A. Rupenyan, J. B. Bertrand, D. M. Villeneuve, and H. J. Wörner, *

1. MODELING AND ANALYSIS OF HIGH-HARMONIC EMISSION FROM TRANSIENT GRATINGS OF ALIGNED MOLECULES

As described in the Letter, the electric field of high-harmonic emission across the transient grating, normalized to the emission of isotropically aligned molecules, is given by

$$\begin{aligned} F(\Omega,x) &= \left[1+\frac{d_\Omega-1}{2}(\sin(kx)+1)\right]\exp\left[i\frac{\phi_\Omega}{2}\{\sin(kx)+1\}\right] \\ &= \left[1+\frac{d_\Omega-1}{2}\sin(kx)+\frac{d_\Omega-1}{2}\right]\exp\left(i\frac{\phi_\Omega}{2}\right)\exp\left[i\frac{\phi_\Omega}{2}\sin(kx)\right] \\ &= \exp\left(i\frac{\phi_\Omega}{2}\right)\left[(1+\frac{d_\Omega-1}{2})\exp\left(i\frac{\phi_\Omega}{2}\sin(kx)\right)+\frac{d_\Omega-1}{2}\sin(kx)\exp\left(i\frac{\phi_\Omega}{2}\sin(kx)\right)\right]. \end{aligned} \tag{1}$$

In the far field, the signal corresponds to the squared modulus of the Fourier transform of $F(\Omega,x)$ with the spatial frequency ξ

$$\mathcal{F}_{x\to\xi}\{F(\Omega,x)\}=\exp\left(i\frac{\phi_\Omega}{2}\right)\sum_{m=-\infty}^{\infty}\left[(1+\frac{d_\Omega-1}{2})J_m(\frac{\phi_\Omega}{2})+i\frac{d_\Omega-1}{4}\{J_{m+1}(\frac{\phi_\Omega}{2})-J_{m-1}(\frac{\phi_\Omega}{2})\}\right]\delta(\xi-m\frac{k}{2\pi}). \tag{2}$$

Here, J_m stands for the m-th order Bessel functions. The analytical form of the Fourier transform has been derived using the following relations,

$$\mathcal{F}\{\sin(kx)\} = \frac{i}{2}\{\delta(\xi+\frac{k}{2\pi})-\delta(\xi-\frac{k}{2\pi})\} \tag{3}$$

$$\mathcal{F}\{\exp(i\frac{\phi_\Omega}{2}\sin(kx))\} = \sum_{m=\infty}^{-\infty}J_m(\frac{\phi_\Omega}{2})\delta(\xi-m\frac{k}{2\pi}) \tag{4}$$

and applying the convolution theorem $\mathcal{F}(A.B)=\mathcal{F}(A)^*\mathcal{F}(B)$:

$$\begin{aligned} \mathcal{F}\{\sin(kx)\exp(i\frac{\phi_\Omega}{2}\sin(kx))\} &= \mathcal{F}\{\sin(kx)\}*\mathcal{F}\left[\exp\{i\frac{\phi_\Omega}{2}\sin(kx)\}\right] \\ &= \frac{i}{2}\{\delta(\xi+\frac{k}{2\pi})-\delta(\xi-\frac{k}{2\pi})\}*\sum_{m=-\infty}^{\infty}J_m(\frac{\phi_\Omega}{2})\delta(\xi-m\frac{k}{2\pi}) \\ &= \frac{i}{2}\sum_{m=-\infty}^{\infty}\left[J_{m+1}(\frac{\phi_\Omega}{2})-J_{m-1}(\frac{\phi_\Omega}{2})\right]\delta(\xi-m\frac{k}{2\pi}). \end{aligned} \tag{5}$$

The periodic modulation of the high-harmonic amplitude and phase in the near field results in several diffraction orders in the far field. The observed intensity distribution in the far field is the power spectrum of Eq. (2) which means that the zeroth order (or non-diffracted) high-harmonic signal has the intensity at the detector

$$I_{m=0}=\left|(1+\frac{d_\Omega-1}{2})J_0(\frac{\phi_\Omega}{2})+i\frac{d_\Omega-1}{4}\{J_1(\frac{\phi_\Omega}{2})-J_{-1}(\frac{\phi_\Omega}{2})\}\right|^2. \tag{6}$$

The first order signal has the intensity

$$I_{m=1}=\left|(1+\frac{d_\Omega-1}{2})J_1(\frac{\phi_\Omega}{2})+i\frac{d_\Omega-1}{4}\{J_2(\frac{\phi_\Omega}{2})-J_0(\frac{\phi_\Omega}{2})\}\right|^2. \tag{7}$$

2. VARIATION OF THE AMPLITUDE AND PHASE OF HIGH-HARMONIC EMISSION FROM ALIGNED N_2 MOLECULES WITH THE DEGREE OF AXIS ALIGNMENT

Here, we theoretically investigate the variation of the amplitude and phase of high-harmonic emission from aligned N_2 molecules with the degree of axis alignment $\langle\cos^2\theta\rangle$. The axis distribution functions $A(\theta)$ used in these calculations are shown in Fig. S1a. The functions corresponding to $\langle\cos^2\theta\rangle = 0.63, 0.60$ and 0.55 result from a solution of the time-dependent Schrödinger equation, reported in Ref. [24] of the letter, fitted to the functional form

$$A(\theta) = N\left(1 + \frac{a}{\cos^2(\theta) + \epsilon^2\sin^2(\theta)}\right) \tag{8}$$

and normalized such that

$$\int_0^\pi A(\theta)\sin\theta \mathrm{d}\theta = 1. \tag{9}$$

The axis distributions corresponding to $\langle\cos^2\theta\rangle = 0.5, 0.44, 0.41$ and 0.33 have been determined by extrapolating the parameters a and ϵ to obtain the desired value of $\langle\cos^2\theta\rangle$.

We calculate the emission at photon energy Ω from an ensemble of molecules aligned at angle α in the laboratory frame according to

$$d_\Omega^\alpha e^{i\phi_\Omega^\alpha} = \int_{\theta'=0}^{\pi}\int_{\phi'=0}^{2\pi}\sqrt{I(\theta)}d_\Omega^\theta e^{i\phi_\Omega^\theta}A(\theta)\sin(\theta')\mathrm{d}\theta'\mathrm{d}\phi', \tag{10}$$

where $\theta = \theta(\theta', \phi'; \alpha)$ is the angle between the polarization axis of the probe field and the internuclear axis, d_Ω^θ and ϕ_Ω^θ are the molecular frame photorecombination dipole amplitudes and phases and the angles are related by the following equation

$$\cos\theta = \cos\alpha\cos\theta' - \sin\alpha\sin\theta'\sin\phi'. \tag{11}$$

Here θ' and ϕ' are the polar and azimuthal angle in the frame about the polarization axis of the aligning pulse. The ionization rate $I(\theta)$ is shown in Fig. S1b.

The emission from an ensemble of aligned molecules is then divided by the emission from the randomly aligned sample, which is obtained from Eq. (10) by setting $A(\theta) = 0.5$. Figure S1c shows the obtained relative phases ϕ_Ω and amplitudes d_Ω of high-harmonic emission in H17-H27 from an ensemble of N_2 molecules aligned under laboratory-frame angles of 0°, 40° and 80° with respect to the polarization of the probe pulse. The variation of both the phases and the amplitudes is found to be close to linear in the range of $\langle\cos^2\theta\rangle = 0.33 - 0.55$, which is relevant to our study. We hence conclude that, in a transient grating of moderately aligned N_2 molecules, the variation of the high-harmonic amplitudes and phases is sinusoidal as assumed in Eq. (1) of the Letter. We expect that this property remains valid for other molecules with highest occupied orbitals of σ symmetry. In the case of π orbitals, sharp phase variations will occur as a function of angle for high degrees of alignment which may cause deviations from linearity. In such cases, higher-order diffraction will be observed and can be used to characterize more complex phase and amplitude variations.

Fig. S2 shows the calculated high-harmonic amplitudes and phases for aligned N_2 molecules, relative to a randomly-aligned sample for different degrees of molecular axis alignment.

* woerner@phys.chem.ethz.ch; www.atto.ethz.ch

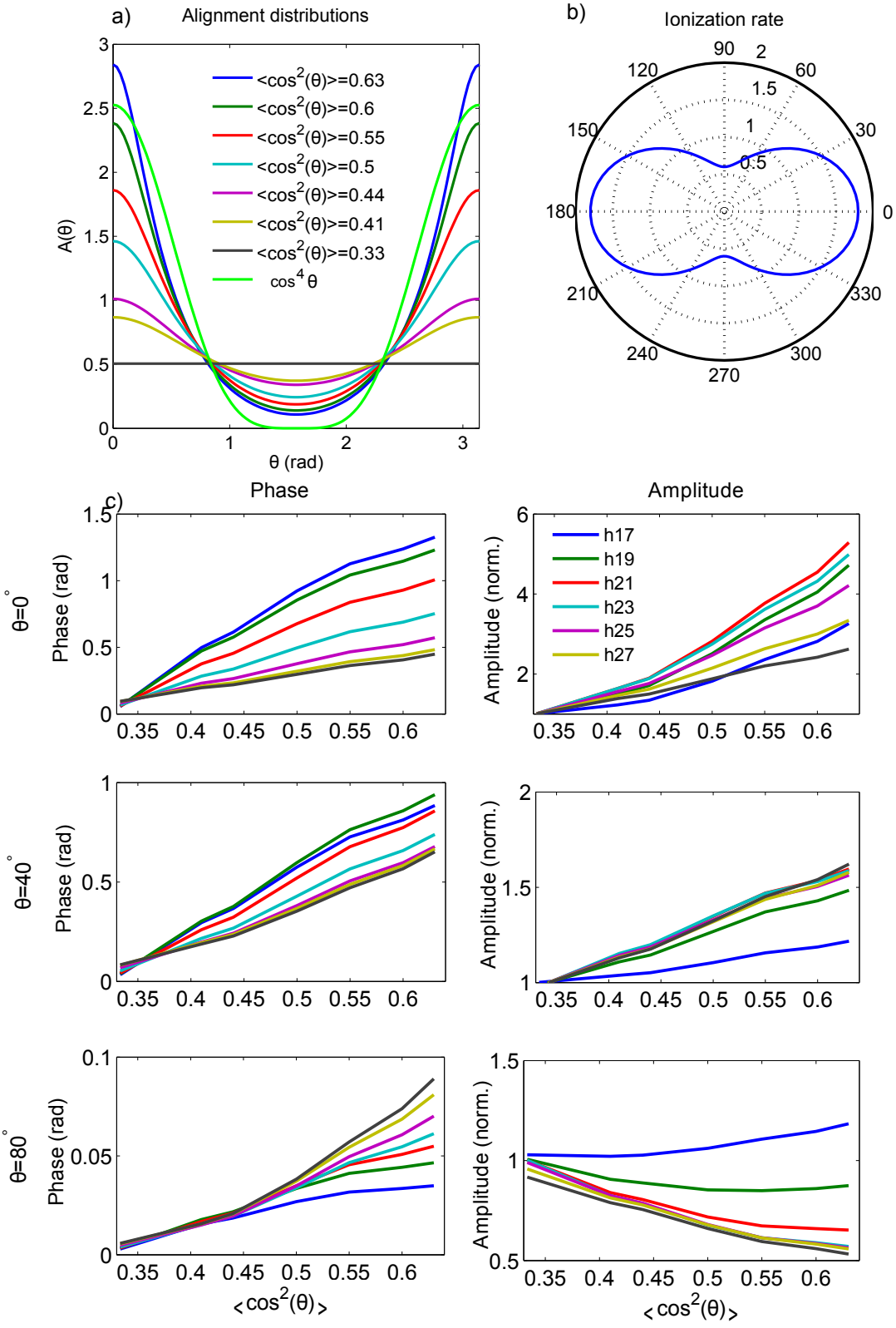

Fig. S1: a) Alignment distributions for different degrees of alignment. b) Strong-field ionization rate of N_2 as a function of the angle between the molecular axis and the probe laser field (from Ref. [23] of the letter). c) Calculated phases and amplitudes for harmonics 17-27 shown as a function of the degree of alignment for three different alignment angles.

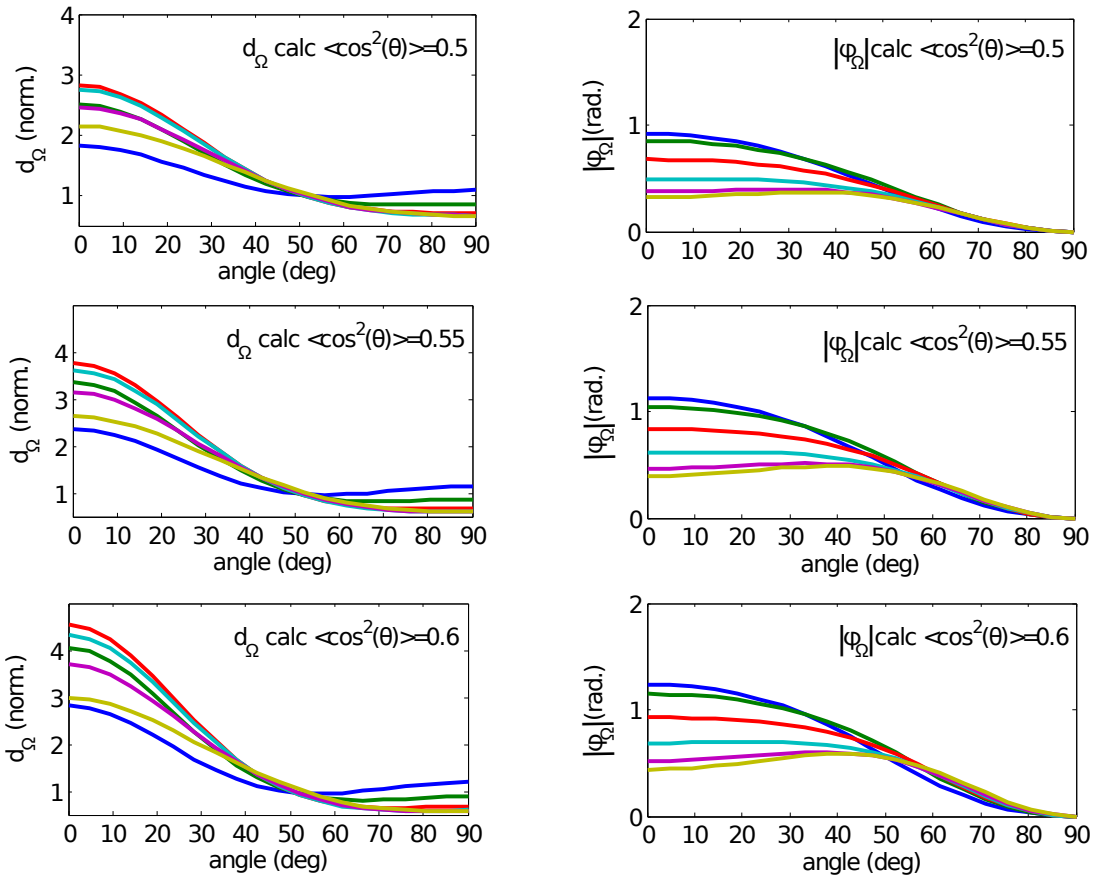

Fig. S2: Calculated high-harmonic amplitudes and phases for aligned N_2 molecules relative to a randomly aligned sample as in Figs. 3c and 3d of the Letter but using three different axis distribution functions shown in Fig. S1a and corresponding to $\langle \cos^2 \theta \rangle = 0.50$, 0.55 and 0.60, respectively.